Acta Biochim Biophys Sin 2013, 45: 953–962 | © The Author 2013. Published by ABBS Editorial Office in association with Oxford University Press on behalf of the Institute of Biochemistry and Cell Biology, Shanghai Institutes for Biological Sciences, Chinese Academy of Sciences. DOI: 10.1093/abbs/gmt096.
Advance Access Publication 12 September 2013

Original Article

MiR-9 reduces human acyl-coenzyme A:cholesterol acyltransferase-1 to decrease THP-1 macrophage-derived foam cell formation

Jiajia Xu[1], Guangjing Hu[1], Ming Lu[1], Ying Xiong[1], Qin Li[1], Catherine C.Y. Chang[2], Baoliang Song[1], Tayuan Chang[2], and Boliang Li[1]*

[1]State Key Laboratory of Molecular Biology, Institute of Biochemistry and Cell Biology, Shanghai Institutes for Biological Sciences, Chinese Academy of Sciences, Shanghai 200031, China
[2]Department of Biochemistry, Geisel School of Medicine at Dartmouth, Hanover, NH 03756, USA
*Correspondence address. Tel: +86-21-54921278; Fax: +86-21-54921279; E-mail: blli@sibcb.ac.cn

MicroRNAs (miRNAs) post-transcriptionally regulate gene expression by targeting mRNAs and control a wide range of biological functions. Recent studies have indicated that miRNAs can regulate lipid and cholesterol metabolism in mammals. Acyl-coenzyme A:cholesterol acyltransferase (ACAT) is a key enzyme in cellular cholesterol metabolism. The accumulated cholesteryl esters are mainly synthesized by ACAT1 during the formation of foam cell, a hallmark of early atherosclerotic lesions. Here, we revealed that miR-9 could target the 3′-untranslated region of human *ACAT1* mRNA, specifically reduce human ACAT1 or reporter firefly luciferase (Fluc) proteins but not their mRNAs in different human cell lines, and functionally decrease the formation of foam cells from THP-1-derived macrophages. Our findings suggest that miR-9 might be an important regulator in cellular cholesterol homeostasis and decrease the formation of foam cells *in vivo* by reducing ACAT1 proteins.

Keywords microRNA; ACAT1; cholesteryl ester; foam cell; atherosclerosis

Received: May 20, 2013 Accepted: June 25, 2013

Introduction

Acyl-coenzyme A:cholesterol acyltransferase (ACAT) also known as sterol O-acyltransferase, consists of two different enzymes (ACAT1 and ACAT2). ACAT catalyzes the formation of cholesteryl esters (CEs) from cholesterol and long-chain fatty acyl-coenzyme A and plays important roles in cellular cholesterol homeostasis [1,2]. Human *ACAT1* cDNA K1 is identified by the functional complementation of mutant Chinese hamster ovary (CHO) cells lacking ACAT activity [3]. It is 4011 bp in length, contains an open reading frame (ORF) of 1650 bp, encodes a protein of 550 amino acids, and has an optional long 5′-untranslated region (5′-UTR) of 1396 bp in length. Its genomic DNA contains 18 exons (exons Xa, Xb, and 1–16); exons 1–16 are located on chromosome 1, whereas exon Xa (1279 bp) is located on chromosome 7 [4]. The origin of mini-exon Xb, which is 10 bp long, is still unclear at present. Northern blot analysis has revealed the presence of four *ACAT1* transcripts (7.0, 4.3, 3.6, and 2.8 kb) in all of the examined human tissue cells and cell lines. Surprisingly, the 4.3-kb *ACAT1* mRNA contains sequences from both chromosomes 1 and 7, indicating that it is produced from two different chromosomes, presumably by an interchromosomal *trans*-splicing event [4].

The chimeric 4.3-kb *ACAT1* mRNA can produce two ACAT1 isoforms (50 kD and 56 kD) [5,6]. Within the optional long 5′-UTR, the secondary RNA structure (nt 1355–1384) is able to enhance the selection of the downstream $AUG_{1397-1399}$ as an initiation codon to produce the 50-kD isoform [7], whereas the two upstream secondary RNA structures (nt 1255–1268 and 1286–1342), transcribed, respectively, from two different chromosomes, are required for producing the 56-kD isoform [6]. Moreover, the optional long 5′-UTR of human *ACAT1* mRNAs impairs the production of ACAT1 protein by promoting its mRNA decay [8]. Up to now, no report has focused on the *ACAT1* mRNA 3′-UTR, which is 934 bp in length and locates in exon 16.

Atherosclerosis and its complications, coronary heart disease, and stroke, constitute the most common cause of mortality, and have become the pre-eminent health problem worldwide during the last decade [9]. Atherosclerosis is a progressive disease characterized by the accumulation of cholesterol and fibrous elements in larger arteries, and is also considered to be a chronic inflammation process [10–13]. The formation of macrophage-derived foam cells that contain massive amounts of CEs becomes a hallmark of early stage of atherosclerotic lesions [10–13]. In macrophages present in human atherosclerotic lesions, a close connection between the foam cell appearance and the ACAT1

protein expression has been demonstrated [1,14]. For instance, the clinical treatment with dexamethasone increases the incidence of atherosclerosis, which may in part be due to enhancing the ACAT1 expression and promoting the accumulation of CEs during the macrophage-derived foam cell formation [15]. Besides, tumor necrosis factor alpha specifically enhances the expression of human *ACAT1* gene through the nuclear factor-kappa B pathway to promote the CE-laden cell formation from the differentiating monocytes [16]. For the reason that ACAT1 is intensively involved in the development of atherosclerosis, ACAT1 has been considered as a drug target for treatment of atherosclerosis [17].

MicroRNAs (miRNAs) are small, non-coding 20−24 nt RNAs that regulate gene expression primarily by binding with an imperfect complementarity to the 3′-UTR of target mRNAs [18−20], leading to translational repression through mRNA degradation and/or translational inhibition [21]. The sequence complementarity between the 6−8 bp seed region of the miRNA and its binding site on the target RNA seems to determine the specificity of miRNA−RNA interactions [22]. miRNAs have emerged as important modulators in multiple normal and disease-related biological processes, including homeostasis [18,20,23,24], oncogenesis [25−27], and cardiogenesis [28,29]. Recent studies have indicated that miRNAs can regulate lipid and cholesterol metabolism in mammals. The overexpression of miR-33 from an sterol regulatory element-binding protein 2 (SREBP2) intron strongly represses ATP-binding cassette sub-family A member 1 (ABCA1) expression at both RNA and protein levels [23,24,30−32], and decreases cellular cholesterol efflux to apolipoprotein A-I, a key step in regulating reverse cholesterol transport [33]. MiR-122 inhibition by antisense oligonucleotides in mice results in the increase of hepatic fatty acid oxidation and the decrease of cholesterol synthesis [33,34]. At present, the effect of miRNAs on the expression of ACAT1, the exclusive enzyme for intracellular CE synthesis, has no report yet.

In this study, we revealed that miR-9 could target 3′-UTR of human *ACAT1* mRNA, specifically reduce human ACAT1 or reporter Fluc proteins but not their mRNAs in different human cell lines, and functionally decrease the formation of foam cells from THP-1-derived macrophages.

Materials and Methods

Prediction of miRNA target

The miRNA targets were predicted using Target Scan 5.1 (http://www.targetscan.org/vert_50/) and PicTar (http://pictar.mdc-berlin.de/).

Cell culture and transfection

All of the cell lines were maintained in a basal medium as indicated, supplemented with 10% fetal bovine serum, 100 μg/ml kanamycin, 50 U/ml streptomycin at 37°C in a humid atmosphere of 5% CO_2 and 95% air. AC29 cells, the mutant CHO cell line lacking endogenous ACAT1, were grown in Ham's F12 medium (Gibco-BRL, Gaithersburg, USA). Human cell line SH-SY5Y was grown in a 1 : 1 mixture of Dulbecco's modified Eagle's medium (DMEM) (Gibco-BRL) and Ham's F12 medium. Human cell line HEK293T was grown in DMEM medium and human monocyte cell line THP-1 cell was grown in RPMI 1640 medium (Gibco-BRL) supplemented with 5% lipoprotein-poor serum. For differentiating into macrophage, THP-1 was cultured with 0.1 μM phorbol 12-myristate 13-acetate (PMA) (Sigma, St Louis, USA) for 48 h. The THP-1-derived macrophage was then incubated with 40 μg/ml oxidized low-density lipoprotein (oxLDL) for another 48 h without PMA for foam cell formation. miRNA mimic was transfected into cells using HiperFect (Qiagen, Hilden, Germany) according to the manufacturer's instructions, or were co-transfected with expression plasmids using Lipofectamine 2000 (Invitrogen, Carlsbad, USA) according to the manufacturer's instructions.

Plasmid construction

First, the expression plasmids for human ACAT1 and reporter Fluc controlled under the human *ACAT1* gene 3′-UTR containing wild-type (pACAT1-W1 and pFluc-W1) and mutated (pACAT1-M1 and pFluc-M1) miR-9 binding sites were constructed. Briefly, the ORFs encoding ACAT1 and reporter Fluc were amplified by polymerase chain reaction (PCR) from plasmids pA1F and pGL3-B with primer sets ACAT1-F/ACAT1-R and Fluc-F/Fluc-R, and inserted into *Nhe*I and *Hin*dIII sites of pcDNA3.1(+) to generate plasmids pACAT1-ORF and pFluc-W1-ORF, respectively. The 3′-UTR of *ACAT1* gene was amplified by PCR from human genomic DNA with primer set W1-F/W1-R, and inserted into *Hin*dIII and *Bam*HI sites of pACAT1-ORF and pFluc-W1-ORF to generate expression plasmids pACAT1-W1 and pFluc-W1. The mutated fragments 3UTR-M1-l and -M1-r were amplified by PCR from the amplified 3′-UTR of *ACAT1* gene with primer sets W1-F/M1-R and M1-F/W1-R, respectively, and then the fragment 3UTR-M1 with mutation of miR-9 binding site (5′-GGTTTC-3′) on 3′-UTR of human *ACAT1* gene was amplified by PCR from a mixture of the two purified fragments 3UTR-M1-l and -M1-r with primer set W1-F/W1-R, and inserted into *Hin*dIII and *Bam*HI sites of pACAT1-W1 and pFluc-W1 to generate expression plasmids pACAT1-M1 and pFluc-M1, respectively.

Then, the expression plasmids for reporter Fluc controlled under the human *ACAT1* gene 3′-UTR containing 3 and 5 tandem wild-type (pFluc-W3 and -W5) and mutated (pFluc-M3 and -M5) miR-9 binding sites were constructed, respectively. Briefly, the wild-type (3UTR-W3-l and -W5-l) and mutated (3UTR-M3-l and -M5-l) fragments were amplified by PCR from the amplified 3′-UTR of *ACAT1* gene with primer sets W1-F/W3-R1, W1-F/W5-R1, W1-F/M3-R2, and W1-F/M5-R2, and inserted into *Hin*dIII and *Nhe*I sites of

pRluc-CMV to generate plasmids p3UTR-W3-l, -W5-l, -M3-l, and -M5-l, respectively. The fragments 3UTR-W-m and -M-m were annealed from complementary oligomer sets W-F1/W-R3 and M-F2/M-R4, and inserted into *Nhe*I and *Xba*I sites of p3UTR-W3-l, -W5-l, -M3-l, and -M5-l to generate plasmids p3UTR-W3-lm, -W5-lm, -M3-lm, and -M5-lm, respectively. The wild-type (3UTR-W3-r and -W5-r) and mutated (3UTR-M3-r and -M5-r) fragments were amplified by PCR from the amplified 3′-UTR of the *ACAT1* gene with primer sets W3-F3/W1-R, W5-F3/W1-R, M3-F4/W1-R, and M5-F4/W1-R, and inserted into *Xba*I and *Bam*HI sites of p3UTR-W3-lm, -W5-lm, -M3-lm, and -M5-lm to generate plasmids p3UTR-W3-lmr, -W5-lmr, -M3-lmr, and -M5-lmr, respectively. The fragments 3UTR-W3-lmr, -W5-lmr, -M3-lmr, and -M5-lmr were obtained by digestion of plasmids p3UTR-W3-lmr, -W5-lmr, -M3-lmr, and -M5-lmr with *Hin*dIII and *Bam*HI, and were inserted into *Hin*dIII and *Bam*HI sites of pFluc-W1 or pFluc-M1 to generate expression plasmids pFluc-W3, -W5, -M3, and -M5, respectively. The primers used for plasmids construction were listed in **Table 1**.

All of the constructed plasmids were confirmed by restriction enzyme digestion and DNA sequencing.

Luciferase assay

Cells were co-transfected with 100 ng reporter luciferase (Firefly luciferase, Fluc) expression plasmids, 10 ng internal control expression plasmid pRluc-CMV (Renilla luciferase, Rluc) plus 50 nM miR-9 mimic or mock miR by Lipofectamine 2000 (Invitrogen) according to the manufacturer's protocol. Forty-eight hours after transfection, the cells were harvested, and the Fluc and Rluc activities were determined using the Dual-Glo Luciferase Assay System (Promega, Madison, USA). The relative reporter Fluc activities were obtained by normalizing the reporter Fluc activities to Rluc activities, and the relative reporter Fluc activities of cells with mock miR transfection were set equal to 1.0 (fold).

RNA isolation, reverse-transcribed-PCR, and quantitative reverse-transcribed-PCR

For miR-9 determination, small RNAs (<200 nt) were prepared from cultured cells by using MirVana™ miRNA Isolation Kit (Ambion, Austin, USA), and reverse-transcribed (RT) using miR-9 specific RT primer. The quantity of miR-9 was determined by quantitative reverse transcribed-PCR (qRT-PCR) using TaqMan MicroRNA Assay Kit (Applied Biosystems, Foster City, USA) in accordance with the manufacturer's instructions, with U6 small nuclear RNA as an internal control. For pri-miR-9s determination, total RNAs were prepared using Trizol (Invitrogen) according to the manufacturer's instructions, and were RT using random primer (Invitrogen). The quantities of three pri-miR-9s were determined by qRT-PCR. For other mRNA determination, total

Table 1 Primers used for plasmids construction

Primer	Primer sequence	Restriction enzyme sites
ACAT1-F	5′-AAAGCTAGCGAGAGCTTCCCGGAGTCGA-3′	*Nhe*I
ACAT1-R	5′-AAGTCCAAGCTTCTAAAACACGTAA-3′	*Hin*dIII
Fluc-F	5′-CTAGCTAGCATGGAAGACGCCAAAAACAT-3′	*Nhe*I
Fluc-R	5′-CCCAAGCTTTTACACGGCGATCTTTCC-3′	*Hin*dIII
W1-F	5′-TAGAAGCTTGGACTTTGTTTCCTCC-3′	*Hin*dIII
W1-R	5′-AAAGGATCCTCAAGAGAAGTCAATATTTATTAGAC-3′	*Bam*HI
M1-F	5′-GAAAGAAAATGTCTGTTTTGGTTTCATAATGTTATACATCCTA-3′	–
M1-R	5′-TAGGATGTATAACATTATGAAACCAAAACAGACATTTTCTTTC-3′	–
W3-R1	5′-AAAGCTAGCTCTTTGGAAAACAGACATTTTCT-3′	*Nhe*I
W5-R1	5′-AAAGCTAGCTCTTTGGAAAACAGACATTTTCTTCTTTGGAAAACAGACATTTTCT-3′	*Nhe*I
M3-R2	5′-AAAGCTAGCTGAAACCAAAACAGACATTTTCT-3′	*Nhe*I
M5-R2	5′-AAAGCTAGCTGAAACCAAAACAGACATTTTCTTGAAACCAAAACAGACATTTTCT-3′	*Nhe*I
W-F1	5′-AAAGCTAGCAGAAAATGTCTGTTTTCCAAAGATCTAGAAAA-3′	*Nhe*I+*Xba*I
W-R3	5′-TTTTCTAGATCTTTGGAAAACAGACATTTTCTGCTAGCTTT-3′	*Nhe*I+*Xba*I
M-F2	5′-AAAGCTAGCAGAAAATGTCTGTTTTGGTTTCATCTAGAAAA-3′	*Nhe*I+*Xba*I
M-R4	5′-TTTTCTAGATGAAACCAAAACAGACATTTTCTGCTAGCTTT-3′	*Nhe*I+*Xba*I
W3-F3	5′-AAATCTAGAAGAAAATGTCTGTTTTCCAAAGA-3′	*Xba*I
W5-F3	5′-AAATCTAGAAGAAAATGTCTGTTTTCCAAAGAAGAAAATGTCTGTTTTCCAAAGA-3′	*Xba*I
M3-F4	5′-AAATCTAGAAGAAAATGTCTGTTTTGGTTTCA-3′	*Xba*I
M5-F4	5′-AAATCTAGAAGAAAATGTCTGTTTTGGTTTCAAGAAAATGTCTGTTTTGGTTTCA-3′	*Xba*I

The mutated nucleotides were underlined.

Table 2 Primers used for qRT-PCR

Gene	Primer	Primer sequence
ACAT1	ACAT1-q-F	5′-GATGAAGGAAGGCTGGTGC-3′
	ACAT1-q-R	5′-GGAAGCTGGTGGCAGTGTAT-3′
Fluc	Fluc-q-F	5′-TCAAAGAGGCGAACTGTGTG-3′
	Fluc-q-R	5′-GGTGTTGGAGCAAGATGGAT-3′
GAPDH	GAPDH-F	5′-ACCCACTCCTCCACCTTTG-3′
	GAPDH-R	5′-CTGTAGCCAAATTCGTTGTCAT-3′
pri-miR-9-1	pri-miR-9-1-F	5′-CTGTATGAGTGGTGTGGAGTCTTC-3′
	pri-miR-9-1-R	5′-TCTCTCCTCCTCTTGTATCCTCTG-3′
pri-miR-9-2	pri-miR-9-2-F	5′-GCTGTATGAGTGTATTGGTCTTCA-3′
	pri-miR-9-2-R	5′-CCTGACCTTTCTGGTTTTTACTGT-3′
pri-miR-9-3	pri-miR-9-3-F	5′-TGTGTCTGTCCATCCCCTCT-3′
	pri-miR-9-3-R	5′-GCACGCAGAAGTTGTGAGAA-3′

RNAs were prepared using Trizol (Invitrogen), followed by removal of residual DNA using DNase I (Promega), and were RT using oligo $(dT)_{18}$. The quantities of *ACAT1*, *Fluc*, and *glyceraldehyde-3-phosphate dehydrogenase (GAPDH)* mRNAs were determined by qRT-PCR using SYBR Green qPCR Master Mix or by PCR and following agarose gel electrophoresis. qRT-PCR and data collection were performed on an Mx3005PTM instrument (Stratagene, La Jolla, USA). The primers used for amplification of pri-miR-9, *ACAT1*, *Fluc*, *and GAPDH* cDNAs were listed in **Table 2**. PCR condition was 95°C for 5 min to activate the DNA polymerase, then 40 cycles of 95°C for 30 s, 60°C for 30 s, and 72°C for 30 s. The melting curves of the PCR products were acquired by a stepwise increase in the temperature from 60 to 95°C after PCR amplification, and the fluorescence was measured with every 1°C increase. The relative *ACAT1* mRNA was obtained by normalizing *ACAT1* mRNA to *GAPDH* mRNA, and the relative *ACAT1* mRNA in cells with mock miR transfection was set equal to 1.0 (fold).

Western blot analysis

Cells were lysed with radioimmunoprecipitation assay lysis buffer [35] containing protease inhibitor mixture (Sigma), and protein concentrations were then determined using the BCA protein assay kit (Bio-Rad, Hercules, USA). Cell lysates were subjected to sodium dodecyl sulfate–polyacrylamide gel electrophoresis for western blot analysis according to a method described previously [16]. After gel separation, the proteins were transferred to nitrocellulose membranes. The membranes were treated at room temperature with 5% milk in tris-buffered saline tween-20 (TBST) (50 mM Tris–HCl, pH 7.6, 0.15 M NaCl, and 0.05% Tween-20) for 3 h, and then incubated with anti-ACAT1 antibody (dilution 1 : 1000; Santa Cruz, Santa Cruz, USA), anti-Fluc antibody (dilution 1 : 1000; Abcam, Cambridge, UK), or anti-β-actin antibody (dilution 1 : 10 000; Sigma) for 3 h, respectively. After incubation with horseradish peroxidase-conjugated secondary antibodies (Pierce, Rockford, USA) for 1 h, the membranes were washed extensively with TBST and Tris-buffered saline (50 mM Tris–HCl, pH 7.6, and 0.15 M NaCl), respectively. The signals were developed using enhanced chemiluminescence western blotting detection reagent (Pierce). The UVP Labwork software (UVP Inc., Upland, USA) was used to quantify band intensities. The ratios of ACAT1 proteins were obtained by normalizing the contents of ACAT1 proteins to those of β-actin proteins, and the ratios of ACAT1 proteins expressed in cells with mock miR transfection were set equal to 1.0 (fold).

Lipid droplet staining

Cells were fixed with 4% formaldehyde for 20 min, rinsed with water, dipped in 60% isopropanol, and stained with Oil red O for 15 min to identify lipid droplets containing CEs. Cell nuclei were then stained in hematoxylin for 3–5 seconds. All of the procedures were performed at room temperature. Lipid droplet accumulation in foam cell was evaluated by Olympus Bx60 microscope and divided into three grades +, ++, and +++, each standing for the intracellular lipid droplet occupying <1/3, 1/3–2/3, or >2/3 in cytoplasm [15,16].

Cholesterol assay

Cellular cholesterol contents were determined using Amplex Red Cholesterol Assay Kit (Molecular Probes/Invitrogen) as described [36] with slight modification. Briefly, for determination of cellular total cholesterol (TC) and free cholesterol (FC), cells were extracted with chloroform/methanol (2 : 1; v/v); the chloroform phase was separated, dried, and dissolved in assay reaction buffer (100 mM potassium phosphate, pH 7.4, 50 mM NaCl, 5 mM cholic acid, and 0.1%

Triton X-100). The content of CE was obtained from the difference of determined TC and FC contents in each sample. The protein amounts were determined by using protein assay kit (Bio-Rad).

Statistical analysis

Western blot and cholesterol assay data were shown as mean ± standard deviation of three independent experiments performed. (**$P < 0.01$, *$0.01 < P < 0.05$, Student's *t*-test).

Other methods

Other molecular biology techniques were performed according to the methods described by Sambrook *et al*. [37].

Results

Prediction of miR-9 target to *ACAT1* mRNA and expression analysis

Up to now, the effect of miRNAs on the expression of ACAT1 has not been reported yet, although many studies have focused on ACAT1 genes or expression [1–8]. Therefore, we used two different computational algorithms, TargetScan 5.1 (http://www.targetscan.org/vert_50/) and PicTar (http://pictar.mdc-berlin.de/) to search the 3′-UTR of human *ACAT1* mRNA for miRNA binding sites. Both algorithms predicted that only miR-9 could target the 3′-UTR of human *ACAT1* mRNA. The predicted miR-9 binding site is located at the 3555–3577 bp region of human *ACAT1* cDNA K1 [**Fig. 1(A)**], and are highly conserved on the 3′-UTR of different *ACAT1* mRNAs from human, chimpanzee, rhesus, rat, mouse, dog, cat, and horse [**Fig. 1(B)**].

In human cells, miR-9 can be matured from three different miR-9 primary transcripts (pri-miR-9s), which are transcribed by genomic loci on chromosomes 1, 5, and 15, respectively [38]. qRT-PCR indicated that among three pri-miR-9s, pri-miR-9-2 was highly expressed especially in THP-1, SH-SY5Y, and SK-N-SH cell lines [**Fig. 1(C)**], while pri-miR-9-1 and pri-miR-9-3 were expressed lowly in all of the human cell lines examined. Also, Caco-2, Huh7, and HepG2 cell lines presented high levels of miR-9 [**Fig. 1(D)**]. Moreover, the levels of human *ACAT1* mRNAs in Caco-2, Huh7, and HepG2 cell lines were lower than those in the other four cell lines examined [**Fig. 1(E)**]. It seems that the levels of miR-9 and *ACAT1* mRNA in human cell lines might appear in a negative correlation.

MiR-9 exogenously reduces human ACAT1 protein but not mRNA

In order to study the effect of miR-9 on the expression of human *ACAT1* gene, we constructed expression plasmids

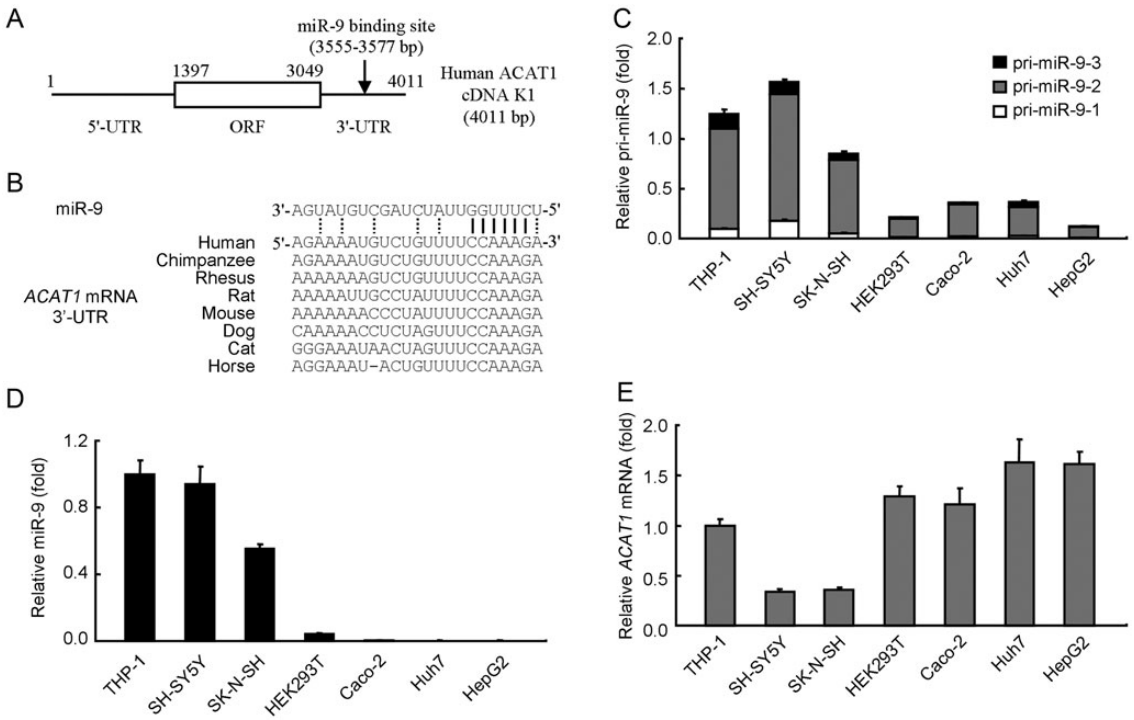

Figure 1 Prediction of miR-9 binding site on *ACAT1* mRNAs and expression analysis (A) Schematic representation of miR-9 binding site on human *ACAT1* cDNA K1. The arrow showed the localization of miR-9 binding site on 3′-UTR. White bar, *ACAT1* gene ORF; horizontal line, 5′- and 3′-UTRs. (B) Prediction of miR-9 binding sites on 3′-UTR of *ACAT1* mRNAs among various species. The vertical solid lines indicated sequence complementarity between the seed region of miR-9 and its binding sites on *ACAT1* mRNAs, and the vertical dotted lines represented the non-seed region complementarity. (C–E) qRT-PCR analysis of the expression of pri-miR-9s (C), miR-9 (D), and human *ACAT1* mRNAs (E) in THP-1, SH-SY5Y, SK-N-SH, HEK293T, Caco-2, Huh7, and HepG2 cells. The relative pri-miR-9-2 (C), miR-9 (D), and *ACAT1* mRNA (E) in THP-1 cells were set as 1.0 (fold), respectively.

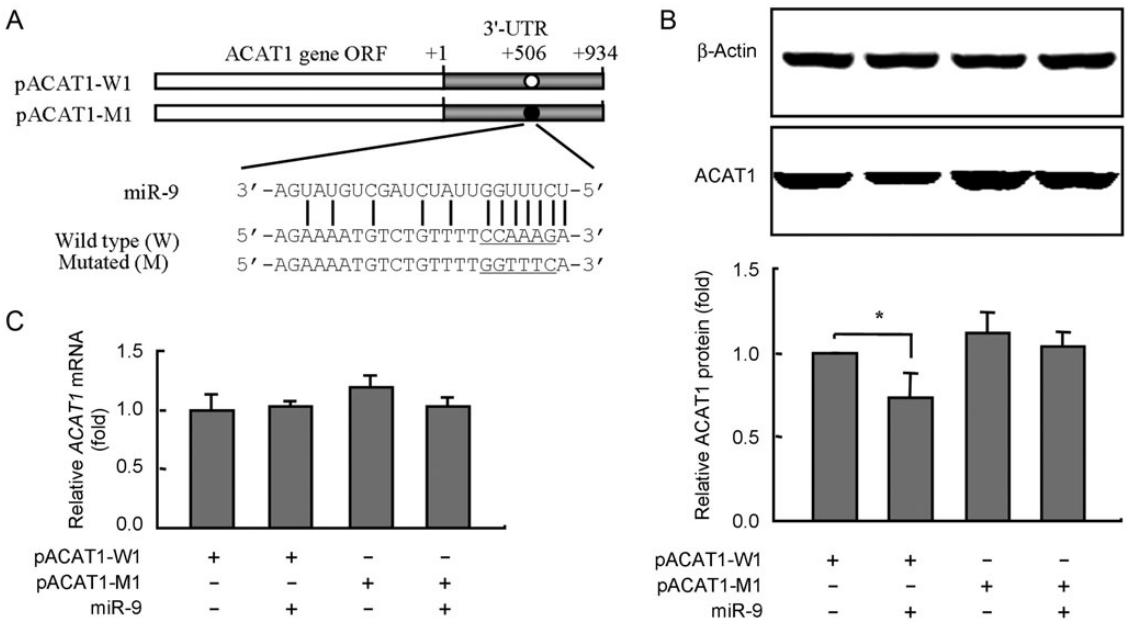

Figure 2 Effect of miR-9 exogenously on the human ACAT1 expression (A) Schematic representation of expression plasmids pACAT1-W1 and pACAT1-M1 with wild-type (5′-CCAAAG-3′) and mutated (5′-GGTTTC-3′) miR-9 binding site on 3′-UTR of human *ACAT1* gene, respectively. White bar, *ACAT1* gene ORF; gray bar, 3′-UTR of human *ACAT1* gene; hollowed circle, wild-type miR-9 binding site; filled circle, and mutated miR-9 binding site. (B,C) AC29 cells were co-transfected with 2 μg pACAT1-W1 or pACAT1-M1 expression plasmid plus 50 nM miR-9 mimic or mock miR per 60-mm dish. Forty-eight hours after transfection, the quantities of ACAT1 proteins were determined by western blot (B; top panel) and the band intensities were quantified by gray scale scan (B; bottom panel), and the quantities of *ACAT1* mRNAs were determined by qRT-PCR (C) and RT-PCR analysis (data not shown). *$0.01 < P < 0.05$.

pACAT1-W1 and pACAT1-M1 with a wild-type (5′-CCAA AG-3′) and mutated (5′-GGTTTC-3′) miR-9 binding site on 3′-UTR of the human *ACAT1* gene, respectively [**Fig. 2(A)**]. Then, AC29 cells were transiently co-transfected with pACAT1-W1 or pACAT1-M1 plus miR-9 mimic or mock miR. Western blot showed that human ACAT1 protein reduced to 73% in cells co-transfected with pACAT1-W1 plus miR-9 mimic compared with that in cells co-transfected with pACAT1-W1 plus mock miR, and no significant change in cells co-transfected with pACAT1-M1 plus miR-9 mimic [**Fig. 2(B)**]. However, at the *ACAT1* mRNA level, no significant effect of miR-9 was observed by qRT-PCR [**Fig. 2(C)**] or agarose gel electrophoresis of RT-PCR products (data not shown). These results showed that miR-9 exogenously reduced human ACAT1 protein but not mRNA.

Attenuation of the reporter Fluc protein by tandem miR-9 binding sites

Next, we constructed a series of expression plasmids for the reporter Fluc controlled under the human *ACAT1* gene 3′-UTR containing 1, 3, or 5 of tandem wild-type (pFluc-W1, 3, or 5) and mutated (pFluc-M1, 3, or 5) miR-9 binding sites [**Fig. 3(A)**]. Luciferase assays showed that when cells were co-transfected with plasmids pFluc-M1, 3, or 5 plus miR-9 mimic, the Fluc activities were decreased (to 83%, 59%, or 30% in SH-SY5Y and to 92%, 65%, or 41% in HEK293T) dependent on the number of tandem miR-9 binding sites [**Fig. 3(B,E)**]. Similarly, western blot indicated that miR-9 reduced reporter Fluc proteins to 78%, 51%, or 29% in SH-SY5Y and to 86%, 50%, or 35% in HEK293T [**Fig. 3(C,F)**]. However, the actions disappeared when miR-9 binding sites were mutated (pFluc-M1, 3, or 5) for luciferase assays [**Fig. 3(B,E)**] and western blot [**Fig. 3(C,F)**]. Further qRT-PCR showed no significant effect of miR-9 on the level of reporter Fluc mRNAs [**Fig. 3(D,G)**]. These results demonstrated that the reporter Fluc was attenuated by tandem miR-9 binding sites on 3′-UTR of human *ACAT1* mRNA.

MiR-9 reduces endogenous ACAT1 protein in different human cell lines

Furthermore, to illustrate whether miR-9 could reduce endogenous ACAT1 protein, SH-SY5Y and HEK293T cells were transfected with miR-9 mimic or mock miR. Western blot showed that endogenous ACAT1 protein was reduced to 78% and 67% in SH-SY5Y and HEK293T cells transfected with miR-9 mimic, respectively, compared with that in cells transfected with mock miR [**Fig. 4(A)**]. However, at the *ACAT1* mRNA level, no significant effect of miR-9 was observed by qRT-PCR [**Fig. 4(B)**] or agarose gel electrophoresis of RT-PCR products (data not shown) in the two human cell lines. The monocytic THP-1 cells can differentiate into macrophage with treatment of PMA, and also the THP-1-derived macrophages can form foam cells under incubation with oxLDL. By transfecting miR-9 mimic or mock miR into THP-1 cells, THP-1-derived macrophages and foam cells, miR-9 resulted in a decrease of ACAT1 proteins to 56%, 68%,

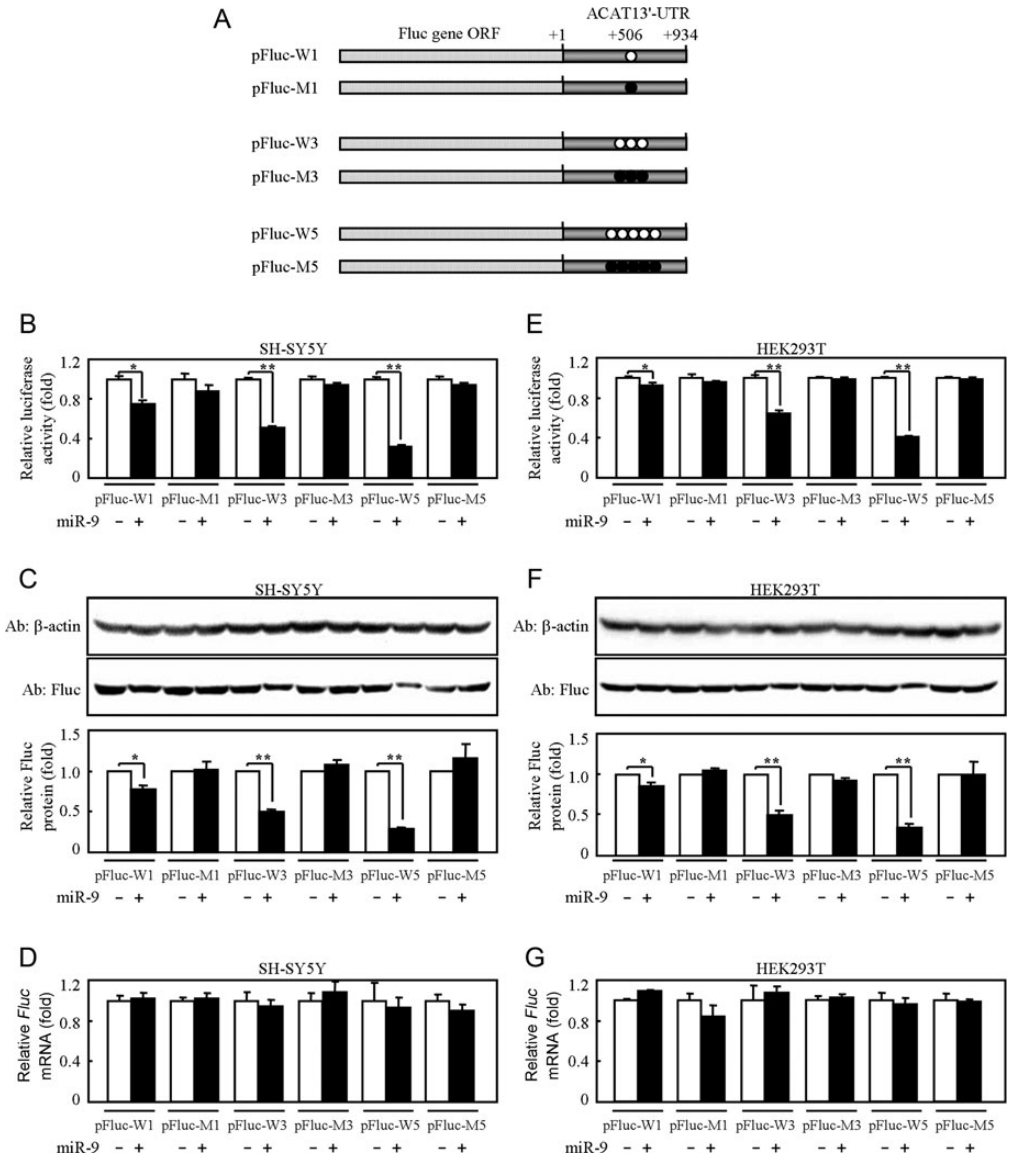

Figure 3 Effect of tandem miR-9 binding sites on the reporter Fluc expression (A) Schematic representation of expression plasmids for the reporter Fluc controlled under the human *ACAT1* mRNA 3′-UTR containing 1, 3, or 5 of tandem wild-type (pFluc-W1, 3, or 5) and mutated (pFluc-M1, 3, or 5) miR-9 binding sites. Dotted bar, *Fluc* gene ORF; gray bar, 3′-UTR of human *ACAT1* gene; hollowed circle, wild-type miR-9 binding site; filled circle, mutated miR-9 binding site. (B–G) SH-SY5Y and HEK293T cells were transfected with 200 ng reporter Fluc expression plasmids as depicted in (A), 20 ng internal control expression plasmid Rluc plus 50 nM miR-9 mimic or mock miR per six-well plate. Forty-eight hours after transfection, the reporter Fluc and internal control Rluc activities were determined using Dual-Glo Luciferase Assay System (B,E), the quantities of reporter Fluc proteins were determined by western blot (C,F; top panel) and the band intensities were quantified by gray scale scan (C,F; bottom panel), and the quantities of reporter *Fluc* mRNAs were determined by qRT-PCR (D,G). $^{**}P < 0.01$, $^{*}0.01 < P < 0.05$.

and 74%, respectively [**Fig. 4(C)**], but no significant effect of miR-9 on the level of *ACAT1* mRNAs [**Fig. 4(D)**]. These results indicated that miR-9 reduced endogenous ACAT1 proteins in different human cell lines including THP-1-derived macrophages and foam cells.

MiR-9 decreases THP-1 macrophage-derived foam cell formation

Since the foregoing results indicated that miR-9 reduced endogenous ACAT1 protein in THP-1-derived macrophages and foam cells, we performed lipid droplet staining and cholesterol assay in detail. The results of lipid droplet staining displayed that the lipid droplets were obviously reduced in THP-1-derived macrophages and foam cells with transfection of miR-9 mimic [**Fig. 5(A)**]. Then, the percentage of foam cells stained at the ++/+++ grades was evaluated. Without the oxLDL treatment, almost no formation of foam cell from THP-1-derived macrophages [**Fig. 5(B)**, lane 1] was observed, whereas with the oxLDL treatment the percentage of foam cells stained at the ++/+++ grades was significantly decreased with transfection of miR-9 mimic [**Fig. 5(B)**, lane 4]. Furthermore, cholesterol assay showed

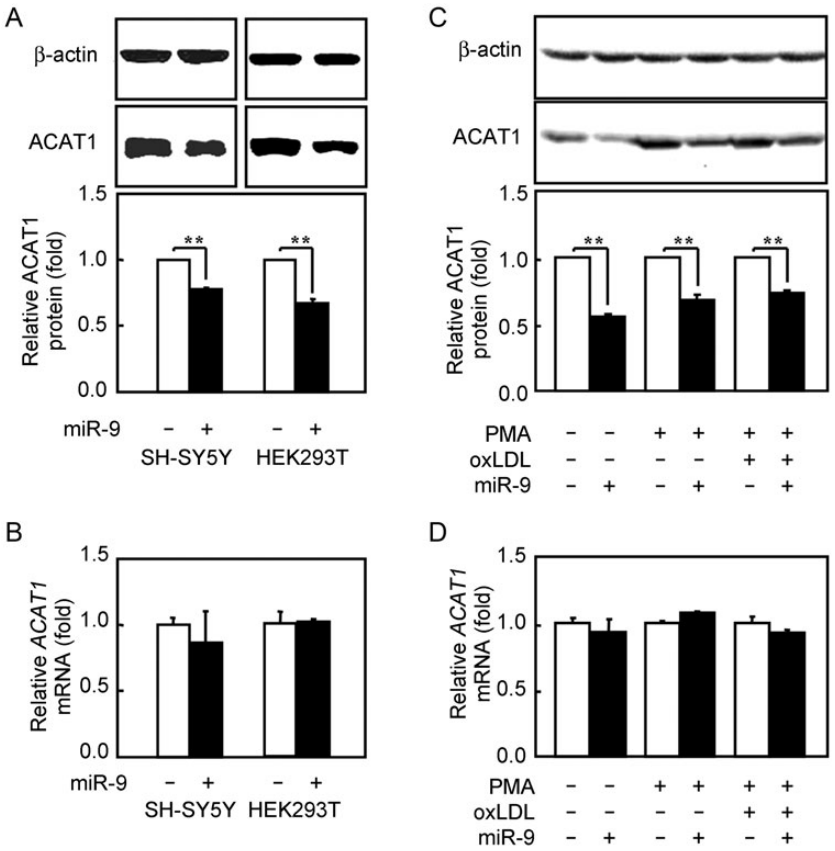

Figure 4 Effect of MiR-9 on the endogenous cellular ACAT1 expression (A,B) SH-SY5Y and HEK293T cells were transfected with 50 nM miR-9 mimic or mock miR per 60-mm dish. The quantities of ACAT1 proteins were determined by western blot (A; top panel) and the band intensities were quantified by gray scale scan (A; bottom panel), the quantities of *ACAT1* mRNAs were determined by qRT-PCR (B) and RT-PCR analysis (data not shown) 48 h after transfection. (C,D) The monocytic THP-1 cells were differentiated into macrophages with a treatment of 0.1 μM PMA for 48 h. THP-1 and THP-1-derived macrophages were transfected with 50 nM miR-9 mimic or mock miR per 60-mm dish, and then THP-1-derived macrophages were incubated with or without 40 μg/ml oxLDL for another 48 h without PMA for further foam cells formation. The quantities of ACAT1 proteins were determined by western blot (C; top panel) and the band intensities were quantified by gray scale scan (C; bottom panel), the quantities of *ACAT1* mRNAs were determined by qRT-PCR (D) and RT-PCR analysis (data not shown) 48 h after transfection. $^{**}P < 0.01$.

that with transfection of miR-9 mimic, the levels of TC and CE were evidently decreased, but FC was not changed [**Fig. 5(C)**]. Significantly, the decreases of CE/TC ratios were observed in THP-1-derived macrophages and foam cells with transfection of miR-9 mimic [**Fig. 5(D)**], which demonstrated that miR-9 reduced ACAT1 proteins followed the enzymatic activities which synthesize the CEs of lipid droplets.

Discussion

In this study, we revealed that miR-9 could target the human *ACAT1* mRNA 3′-UTR, which contains a miR-9 binding site located at the 3555–3577 bp region corresponding to human *ACAT1* cDNA K1 [**Fig. 1(A)**], and specifically reduced human ACAT1 or reporter Fluc proteins but not their mRNAs in different human cell lines (**Figs. 2–4**). In the beginning, the results showed that the levels of miR-9 and *ACAT1* mRNA in human cell lines may appear in a negative correlation [**Fig. 1(D,E)**]. Further studies demonstrated that miR-9 specifically reduces proteins but not mRNAs (**Figs. 2–4**). Hence, the reductive effect of miR-9 observed is mainly through inhibition of the protein translation, which is one of two identified independent mechanisms of miRNA silencing [21]. At present, the possibility of ACAT1 protein degradation has not been ruled out.

Furthermore, the lipid droplet staining and cholesterol assay showed that miR-9 could functionally decrease the formation of foam cells from THP-1-derived macrophages by reducing ACAT1 proteins following the enzymatic activities, which synthesize the CEs of lipid droplets [**Fig. 4(C)** and **Fig. 5**]. The obtained data suggest that miR-9 might be an important regulator in cellular cholesterol homeostasis and decrease the formation of foam cells *in vivo*, a hallmark of early atherosclerotic lesions, by reducing ACAT1 proteins. In fact, several studies have been conducted on the expression of miR-9 in monocytic cells including human primary monocyte and THP-1 cell line with the oxLDL treatment [39,29], but no functional target of miR-9 in cellular cholesterol homeostasis has been characterized yet. Therefore, our

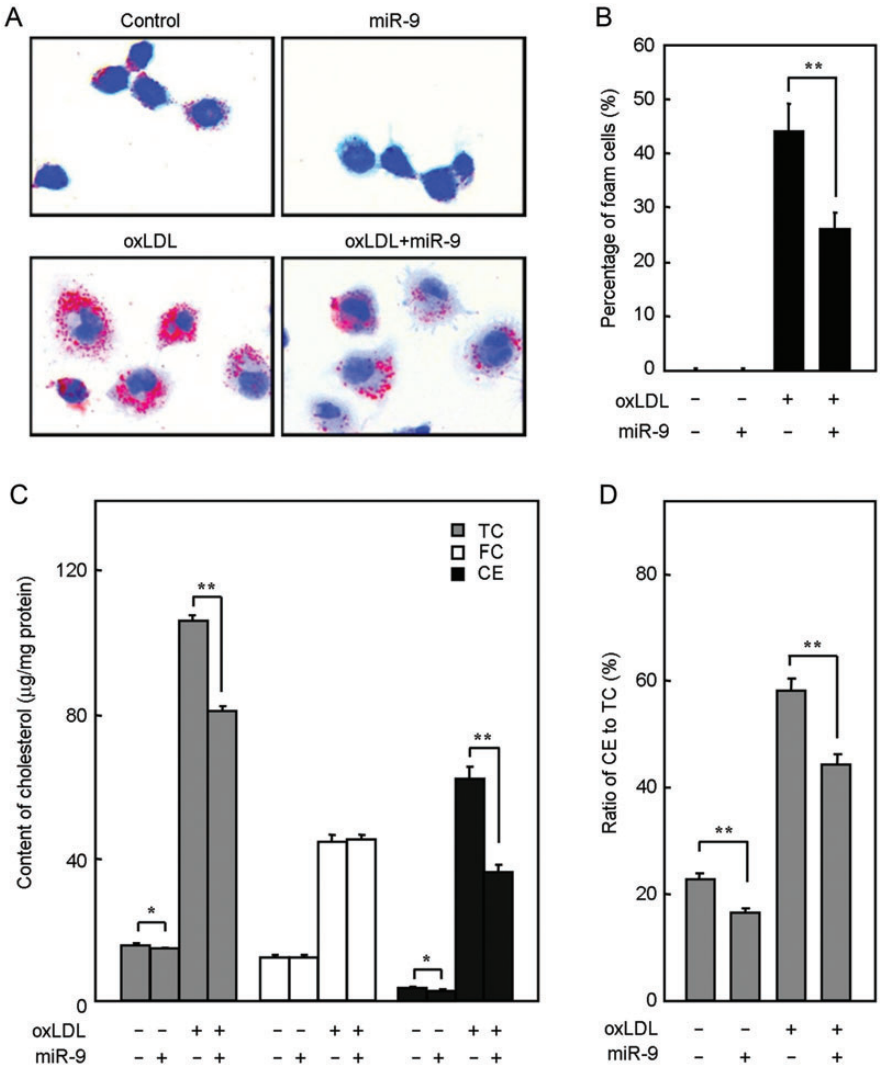

Figure 5 Action of miR-9 on foam cell formation from THP-1-derived macrophages The monocytic THP-1 cells differentiated into macrophages with a treatment of 0.1 μM PMA for 48 h, and THP-1-derived macrophages were transfected with 50 nM miR-9 mimic or mock miR, and then incubated with or without 40 μg/ml oxLDL for another 48 h without PMA for further foam cells formation. (A,B) The lipid droplets in the treated cells were stained with Oil red O, and cell nuclei were counterstained with Meyer's hematoxylin. Representative lipid droplet staining images were shown in (A), and the percentage of foam cells stained at the ++/+++ grades was shown in (B). (C,D) The contents of cellular TC and FC were determined by cholesterol assay, and the contents of CE were obtained from the difference of determined TC and FC contents in each sample. The contents of TC, FC, and CE in each sample were shown in (C), and the ratios of CE to TC (%) were shown in (D). $^{**}P < 0.01$, $^{*}0.01 < P < 0.05$.

findings may provide a new highlight that miR-9 may down-regulate the human ACAT1 and prevent the formation of foam cells at an early stage of atherosclerosis.

Interestingly, when THP-1-derived macrophage was transfected with miR-9 mimic and incubated with oxLDL for foam cell formation, the levels of TC and CE were evidently decreased while FC was not changed [**Fig. 5(C)**]. This phenomenon might be due to the efflux acceleration and influx slowdown of cellular cholesterols, and therefore, should be further studied to illustrate other proteins, such as low-density lipoprotein receptor, cluster of differentiation 36, ABCA1, and ATP-binding cassette sub-family G member 1/4 which may be involved in this process.

Funding

This work was supported by grants from the Ministry of Science and Technology of China (2011CB910900 and 2009CB919000).

References

1 Chang TY, Chang CC and Cheng D. Acyl-coenzyme A:cholesterol acyltransferase. Annu Rev Biochem 1997, 66: 613–638.
2 Chang TY, Li BL, Chang CC and Urano Y. Acyl-coenzyme A:cholesterol acyltransferases. Am J Physiol Endocrinol Metab 2009, 297: E1–E9.
3 Chang CC, Huh HY, Cadigan KM and Chang TY. Molecular cloning and functional expression of human acyl-coenzyme A:cholesterol acyltransferase

cDNA in mutant Chinese hamster ovary cells. J Biol Chem 1993, 268: 20747–20755.
4 Li BL, Li XL, Duan ZJ, Lee O, Lin S, Ma ZM and Chang CC, *et al*. Human acyl-CoA:cholesterol acyltransferase-1 (ACAT-1) gene organization and evidence that the 4.3-kilobase ACAT-1 mRNA is produced from two different chromosomes. J Biol Chem 1999, 274: 11060–11071.
5 Yang L, Lee O, Chen J, Chen J, Chang CC, Zhou P and Wang ZZ, *et al*. Human acyl-coenzyme A:cholesterol acyltransferase 1 (acat1) sequences located in two different chromosomes (7 and 1) are required to produce a novel ACAT1 isoenzyme with additional sequence at the N terminus. J Biol Chem 2004, 279: 46253–46262.
6 Chen J, Zhao XN, Yang L, Hu GJ, Lu M, Xiong Y and Yang XY, *et al*. RNA secondary structures located in the interchromosomal region of human ACAT1 chimeric mRNA are required to produce the 56 kDa isoform. Cell Res 2008, 18: 921–936.
7 Yang L, Chen J, Chang CC, Yang XY, Wang ZZ, Chang TY and Li BL. A stable upstream stem-loop structure enhances selection of the first 5′-ORF-AUG as a main start codon for translation initiation of human ACAT1 mRNA. Acta Biochim Biophys Sin 2004, 36: 259–268.
8 Zhao X, Chen J, Lei L, Hu G, Xiong Y, Xu J and Li Q, *et al*. The optional long 5′-untranslated region of human ACAT1 mRNAs impairs the production of ACAT1 protein by promoting its mRNA decay. Acta Biochim Biophys Sin 2009, 41: 30–41.
9 Rosamond W, Flegal K, Friday G, Furie K, Go A, Greenlund K and Haase N, *et al*. Heart disease and stroke statistics 2007 update: a report from the American Heart Association Statistics Committee and Stroke Statistics Subcommittee. Circulation 2007, 115: e69–e171.
10 Lusis AJ. Atherosclerosis. Nature 2000, 407: 233–241.
11 Libby P. Inflammation in atherosclerosis. Nature 2002, 420: 868–874.
12 Hansson GK, Robertson AK and Söderberg-Nauclér C. Inflammation and atherosclerosis. Annu Rev Pathol 2006, 1: 297–329.
13 Glass CK and Witztum JL. Atherosclerosis: the road ahead. Cell 2001, 104: 503–516.
14 Miyazaki A, Sakashita N, Lee O, Takahashi K, Horiuchi S, Hakamata H and Morganelli PM, *et al*. Expression of ACAT-1 protein in human atherosclerotic lesions and cultured human monocytes-macrophages. Arterioscler Thromb Vasc Biol 1998, 18: 1568–1574.
15 Yang L, Yang JB, Chen J, Yu GY, Zhou P, Lei L and Wang ZZ, *et al*. Enhancement of human ACAT1 gene expression to promote the macrophage-derived foam cell formation by dexamethasone. Cell Res 2004, 14: 315–323.
16 Lei L, Xiong Y, Chen J, Yang JB, Wang Y, Yang XY and Chang CC, *et al*. TNF-alpha stimulates the ACAT1 expression in differentiating monocytes to promote the CE-laden cell formation. J Lipid Res 2009, 50: 1057–1067.
17 Li BL, Chang TY, Chen J, Chang CC and Zhao XN. Human ACAT1 gene expression and its involvement in the development of atherosclerosis. Future Cardiol 2006, 2: 93–99.
18 Bartel DP. MicroRNAs: genomics, biogenesis, mechanism, and function. Cell 2004, 116: 281–297.
19 Ambros V. The functions of animal microRNAs. Nature 2004, 431: 350–355.
20 Filipowicz W. RNAi: the nuts and bolts of the RISC machine. Cell 2005, 122: 17–20.
21 Behm-Ansmant I, Rehwinkel J and Izaurralde E. MicroRNAs silence gene expression by repressing protein expression and/or by promoting mRNA decay. Cold Spring Harb Symp Quant Biol 2006, 71: 523–530.
22 Lewis BP, Burge CB and Bartel DP. Conserved seed pairing, often flanked by adenosines, indicates that thousands of human genes are microRNA targets. Cell 2005, 120: 15–20.
23 Najafi-Shoushtari SH, Kristo F, Li Y, Shioda T, Cohen DE, Gerszten RE and Näär AM. MicroRNA-33 and the SREBP host genes cooperate to control cholesterol homeostasis. Science 2010, 328: 1566–1569.
24 Rayner KJ, Suárez Y, Dávalos A, Parathath S, Fitzgerald ML, Tamehiro N and Fisher EA, *et al*. MiR-33 contributes to the regulation of cholesterol homeostasis. Science 2010, 328: 1570–1573.
25 Medina PP and Slack FJ. MicroRNAs and cancer: an overview. Cell Cycle 2008, 7: 2485–2492.
26 Zhang B, Pan X, Cobb GP and Anderson TA. MicroRNAs as oncogenes and tumor suppressors. Dev Biol 2007, 302: 1–12.
27 Drakaki A and Iliopoulos D. MicroRNA gene networks in oncogenesis. Curr Genomics 2009, 10: 35–41.
28 Wang K, Long B, Zhou J and Li PF. MiR-9 and NFATc3 regulate myocardin in cardiac hypertrophy. J Biol Chem 2010, 285: 11903–11912.
29 Chen T, Huang Z, Wang L, Wang Y, Wu F, Meng S and Wang C. MicroRNA-125a-5p partly regulates the inflammatory response, lipid uptake, and ORP9 expression in oxLDL-stimulated monocyte/macrophages. Cardiovasc Res 2009, 83: 131–139.
30 Marquart TJ, Allen RM, Ory DS and Baldán A. MiR-33 links SREBP-2 induction to repression of sterol transporters. Proc Natl Acad Sci USA 2010, 107: 12228–12232.
31 Gerin I, Clerbaux LA, Haumont O, Lanthier N, Das AK, Burant CF and Leclercq IA, *et al*. Expression of miR-33 from an SREBP2 intron inhibits cholesterol export and fatty acid oxidation. J Biol Chem 2010, 285: 33652–33661.
32 Horie T, Ono K, Horiguchi M, Nishi H, Nakamura T, Nagao K and Kinoshita M, *et al*. MicroRNA-33 encoded by an intron of sterol regulatory element-binding protein 2 (Srebp2) regulates HDL in vivo. Proc Natl Acad Sci USA 2010, 107: 17321–17326.
33 Rotllan N and Fernández-Hernando C. MicroRNA regulation of cholesterol metabolism. Cholesterol 2012; (Epub 5 August 2012).
34 Esau C, Davis S, Murray SF, Yu XX, Pandey SK, Pear M and Watts L, *et al*. MiR-122 regulation of lipid metabolism revealed by in vivo antisense targeting. Cell Metab 2006, 3: 87–98.
35 Tang JJ, Li JG, Qi W, Qiu WW, Li PS, Li BL and Song BL. Inhibition of SREBP by a small molecule, betulin, improves hyperlipidemia and insulin resistance and reduces atherosclerotic plaques. Cell Metab 2011, 13: 44–56.
36 Huttunen HJ, Greco C and Kovacs DM. Knockdown of ACAT-1 reduces amyloidogenic processing of APP. FEBS Lett 2007, 581: 1688–1692.
37 Sambrook J, Fritsch EF and Maniatis T. Molecular Cloning. 2nd edn. New York: Cold Spring Harbor Laboratory Press, 1989.
38 Laneve P, Gioia U, Andriotto A, Moretti F, Bozzoni I and Caffarelli E. A minicircuitry involving REST and CREB controls miR-9-2 expression during human neuronal differentiation. Nucleic Acids Res 2010, 38: 6895–6905.
39 Forrest AR, Kanamori-Katayama M, Tomaru Y, Lassmann T, Ninomiya N, Takahashi Y and de Hoon MJ, *et al*. Induction of microRNAs, mir-155, mir-222, mir-424 and mir-503, promotes monocytic differentiation through combinatorial regulation. Leukemia 2010, 24: 460–466.